Modelling for Interior Faults of Induction Motors and Its Simulation on EMTDC

Zexiang Cai[1], Aiyun Gao[1], and Jiandong Jiang[1]

(1) Electric Power College, South China University of Technology, Guangzhou, 510640, China(e-mail: epzxcai@scut.edu.cn, gaoaiyun_hg@sohu.com, dlxy_jjd@163.net)

Abstract – **Based on the fact that induction motor parameters change when there is interior faults, this paper provides one type of interior faults models and uses the electro-magnetic transient simulation software EMTDC to verify the models. The spectrum of steady stator current contains the component lower 2sf (s is the slip) than the fundamental frequency after bars break. Similarly, according to the Extended Park's Vector Approach (EPVA), the spectrum of steady stator current Park's Vector modulus includes 2f component. By the above two characteristic frequency components this paper compares the simulating results with the experimental data and proves interior faults models are correct. Therefore, it makes interior faults study accurate to the extent of every turn, every bar and completes quantitative simulating study on interior faults of induction motors. At the same time, it enriches interior faults models of induction motors in EMTDC and extends its application function and field.**

Keywords – interior faults models, EMTDC, EPVA

I. INTRODUCTION

The interior fault of induction motors account for the proportion almost more than 70% of induction motor failures. It is a key problem to find a quantificational analysis tool for studying the diagnosis and protection of induction motor faults. Conventional methods make use of the test machines, however, the machines have to be damaged to complete the experiments of interior fault. It is always difficult to do experiments repeatedly and to proceed on larger capacity motors. Based on EMTDC (EMTP), this paper presents simulation models and methods for interior faults, including both stator and rotor faults of induction motors, establishing a simulating analysis environment for the research of induction motors' interior faults.

The induction motor model in EMTDC is basically the same as the model in EMTP and both use the H.W. Dommel model. At present, EMTDC gives all kinds of component models of 3-phase induction motors. The accurate extent is only to the induction motor end, so it is applicable to analyze all types of external failures, mechanical (start-up, regulating speed) characteristic, etc., but it can't deal with interior faults such as broken bars, turn-to-turn faults and so on. The efforts in this paper are to enrich interior faults analytical models, and application fields of EMTDC (EMTP) would be extended. This paper compares the simulation results with the experimental data and verifies the models and methods are correct.

II. MOTOR MODELS IN EMTDC AND METHOD OF INTERIOR FAULTS SIMULATION

Induction motors models in EMTDC are constructed by transforming the rotor into three-phase windings that winding coefficient and every phase turns in series are same to those in stator, then continuing Park's Transform and equivalent circuit transform, and simplifying into impedance in parallel with current source. Induction motor model in EMTDC have no inherent mechanical model. It transforms mechanical parts into concentrated R-L-C equivalent network and as one part of the whole electrical network to make solutions. The electric torque is regarded as current source injecting the network. Refer to [2] about the electrical and mechanical models in details.

The above have mentioned that induction motor model itself in EMTDC can't deal with interior stator and rotor faults. However, according to the machine theory interior faults of induction motors will cause changes of corresponding parameters. If we can find the quantitative relation among machine parameters, fault types and fault extent, we are able to indirectly reflect interior faults by setting parameter changes of induction motor model in EMTDC. This is the method of interior faults modeling based on EMTDC simulating.

Rotor models of induction motor in EMTDC include wound rotor and squirrel cage. Squirrel cage motors cover single and double cage. The differences between wound rotor and squirrel cage rest with that the wound rotor can connect outer impedance whereas squirrel cage can't. However, we find that wound rotor may substitute for squirrel cage rotor which impedance parameters are the same, and simulating results are very similar whether under normal state or at failure state (Table I). This provides one simulating environment based on EMTDC for modeling broken bars faults and etc. by changing rotor parameters.

Another limit to induction motors in EMTDC is that its stator and rotor parameters are supposed symmetrical. In fact, for interior faults of induction motors just the asymmetry of stator or rotor result in diversified electrical and mechanical failure characteristics. Thus this paper further verifies placing the rotor impedance of wound rotor inside induction motors (as machine parameters) or connecting to rotor ends (as outer impedance) is equivalent. See Table I. So we can simulate the rotor asymmetry by connecting corresponding impedance to wound rotor ends. Similarly, this paper also validates that placing the stator impedance

inside or outside is equivalent and we can embody the stator asymmetry by the corresponding outer stator impedance. See Table II.

III. MODEL FOR INTERIOR FAULTS OF INDUCTION MOTORS

A. Broken Bar Fault of Squirrel Cage Motor

It is required that the model of broken bar faults should reflect the broken bar amount and various locations of broken bars, however, this process is very complicated. As a matter of fact, we often simplify the model [3]. For example, only considering the greatly possible broken bar failure, that is, with one broken bar adjacent bars are prone to break due to the increase of current. Suppose that Z_2 is the number of rotor bars and n is broken bars. The assumptions of the model produced in this paper as follows.

- n Smooth surfaces of both stator and rotor, stator windings with sinusoidal distributions, saturation and iron losses neglected,
- n Concentrated rotor bars, small broken bar number (much less than the bar/pole number), rotor impedance localized in the bars,
- n Slip value near the rated one.

On the basis of the above assumption, a cage rotor with n broken bars can be analyzed as a three phase wound rotor with a phase affected by an impedance increasing ΔZ ($\Delta Z = \Delta R / s + j\Delta X$)dependant on the broken bar number. This means to neglect the difference in the mutual linkage inductance coefficients between different windings.

Suppose rotor has Z_2 bars and n broken bars. The correlation of ΔR, ΔX and n as follows [4].

Under normal condition, the transformation value of rotor resistance is

$$R_2^{'} \approx r_w \left(\frac{K_B l_B}{A_B} + \frac{Z_2 D_R}{2pp^2 A_R} \right) \frac{4m_1 (N_1 k_{N1})^2}{Z_2}$$
$$= R_B^{'} + R_R^{'} \tag{1}$$

Obviously only Z_2 is related to $R_B^{'}$.

The p.u. of rotor linkage inductance is

$$X_{d2}^{*} = X_{s2}^{*} + X_{d2}^{*} + X_{E2}^{*} + X_{sk}^{*} \tag{2}$$

The transformation value of rotor resistance after failure is

$$R_{2f}^{'} \approx R_{Bf}^{'} + R_{Rf}^{'} = \frac{Z_2}{Z_2 - n} R_B^{'} + R_R^{'} \tag{3}$$

So,

$$\Delta R = R_{2f}^{'} - R_2^{'} = \frac{n}{Z_2 - n} R_B^{'} \approx \frac{n}{Z_2} R_B^{'} \tag{4}$$

In the same way we get

$$\Delta X = \frac{n}{Z_2 - n} X_{s2}^{*} + \frac{(\sum R)_f}{\sum R} (X_{d2}^{*} + X_{sk}^{*}) \tag{5}$$

By the above formula the author compute the Y90S-4 induction motor and obtain rotor impedances before and after broken bar failure. See Table III.

Table III show that rotor impedances indeed increase after the bar breaks and the broken bar failure can be simulated by connecting impedance increasing ΔZ to the rotor ends. It is noticed that the model doesn't cover the affect of the bar configure, that is, the distribution coefficient of rotor bar.

B. Turn-to-turn Failure of Stator

The modeling method of the turn-to-turn stator failure is similar to the broken bar fault, that is, the turn-to-turn stator failure is modeled by symmetrical three phase windings with the failure phase influenced by the corresponding ΔZ ($\Delta Z = \Delta R + j\Delta X$). The computation of ΔZ as follows[4]:

Under well-balanced condition the stator resistance is

$$R_1 = r_w \frac{2N_1 l_c}{N_{t1} A_{c1} a_1} \tag{6}$$

The p.u. of stator linkage inductance is

$$X_{d1}^{*} = X_{s1}^{*} + X_{d1}^{*} + X_{E1}^{*} \tag{7}$$

Assuming M turns are shorted, substituting $N_1^{'} = N_1 - M$ for N_1 in the above two formula we acquire the stator parameter after fault, and then ΔZ.

Table IV is the comparison of stator impedances with different turn-to-turn faults in B phase for Y90S-4 Type machine. The ratio of shorted turns is defined as the percent of shorted turns over the whole branch turns [5]. It is obvious that stator impedances decrease due to the turn-to-turn failure and the decreased value increases with the augment of shorted turn ratio.

IV. EXAMPLE OF SIMULATION

In this paper the Y90S-4 Type machine is simulated. Its rated voltage is 380V, rated power 1.1kW, rated current 2.7A, rated slip 6.47%, efficiency 78%, power factor 0.78, started current time 6.5, started torque time 2.2, the most torque time 2.2. The load of motor with shorted turns is 30% and full under the broken bar condition.

According to the above model the author simulate interior faults and get the spectrum of steady stator current.

The spectrum of steady stator current under shorted turns condition in B phase with 30% is showed in Fig. 1 to 4. Fig. 5 and 6 are the spectrum of steady stator current under two broken bars condition with full load. And the spectrum of steady stator current for one broken bar failure with full load can be found in Fig.7.

V. ANALYSIS OF SIMULATION RESULTS

Due to shorted turns the stator current isn't symmetrical any more. Considering that stator windings have no neutral connection, the motor stator current can be expressed as the sum of a positive- and negative-sequence component. The presence of the negative current manifests itself in the EPVA signature by the presence of a spectral component at twice the fundamental supply frequency($2f_1$)[5]. More-over, the amplitude of this spectral component is directly related to the extension of the fault. In this way, an

Table I: The verifying results of rotor

Verifying contents / Type of rotor	Stator current (Unit: A) / relative error				
	Rated	Single-phase fault	Interior 50% and outer 50% of rotor parameters	Interior 80% and outer 20% of rotor parameters	Interior 20% and outer80% of rotor parameters
Wound rotor	2.5851 /0	4.4316 /0	2.6071 /0.85%	2.5940 /0.34%	2.6199 /1.35%
Squirrel cage rotor	2.5731 /0.46%	4.4400 /0.19%			

Table II: The verifying results of stator

Verifying contents / operation condition	Stator current (Unit: A)/ relative error			
	Interior 100% stator impedance	Interior 50% and outer 50% of stator impedance	Interior 80% and outer 20% of stator impedance	Interior 20% and outer 80% of stator impedance
Rated operation	2.5684 /0	2.5800 /0.45%	2.5726 /0.16%	2.5883 /0.77%
Single-phase fault	23.6860 /0	23.7219 /0.15%	23.7001 /0.06%	23.7444 /0.25%

Table III: The impedances of rotor before and after broken bars

Operation condition / motor parameter	Before broken bar	One broken bar	Two broken bar
Resistance (p.u.)	0.0692	0.072	0.075
Inductance (p.u.)	0.1161	0.1331	0.1441

Table IV: The impedances of stator before and after inter-turn stator winding fault

Operation condition / motor parameter	Well-balanced	Shorted ratio is 2%	Shorted ratio is 8%	Shorted ratio is 24.5%	Two turns shorted
Resistance(p.u.)	0.0836	0.082	0.0768	0.0632	0.083
Inductance(p.u.)	0.0877	0.0845	0.0742	0.0501	0.0865

Fig. 1: The spectrum of stator current Expended
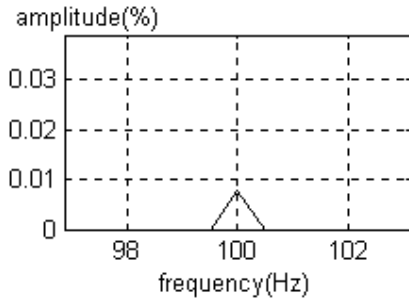
Park's modulus with two turns shorted

Fig. 2: The spectrum of stator current Expended
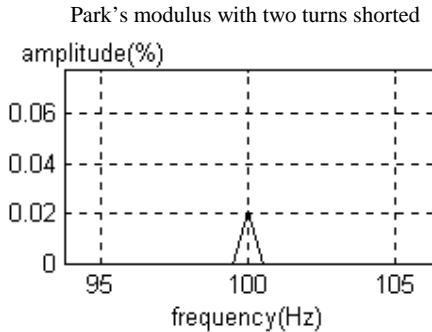
Park's modulus with 2% turns shorted

Fig. 3: The spectrum of stator current Expended
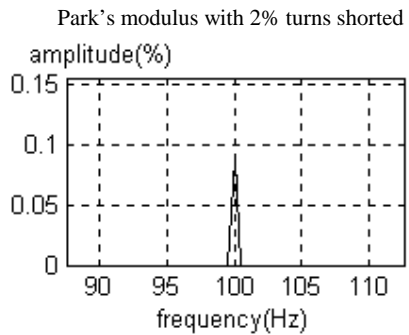
Park's modulus with 8% turns shorted
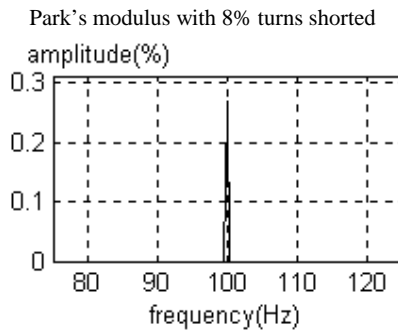
Fig.4: The spectrum of stator current Expended

Park's modulus with 24.5% turns shorted
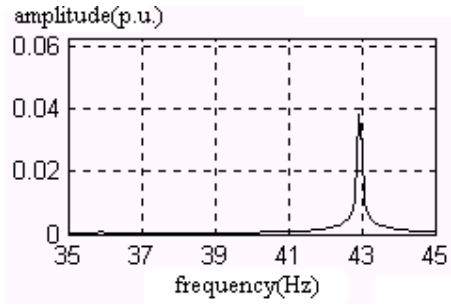
Fig. 5: The spectrum of steady stator current

with two broken bars(simulating)

Fig. 6: The spectrum of steady stator current

with two broken bars (testing)
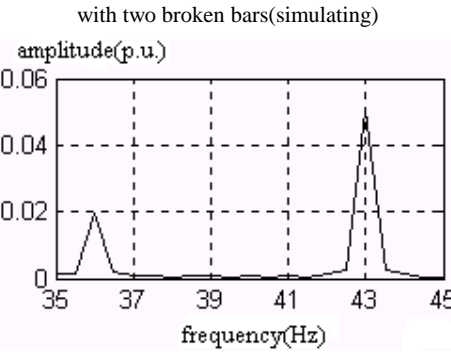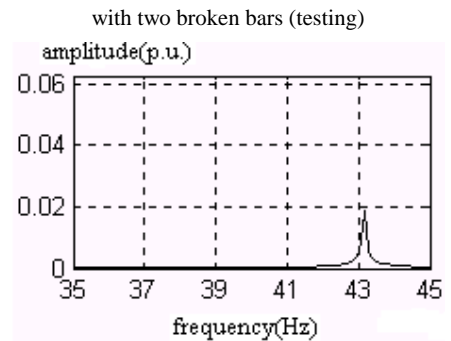
Fig.7: The spectrum of steady stator current

with one broken bar(simulating)

indicator of the degree of asymmetry can be obtained as the ratio between the amplitude of the spectral component at a frequency of $2f_1$ and the dc level of the current Park's Vector. Therefore, the detection of shorted turns failure is completed. The simulating results show that the existence of a spectral component at twice the fundamental supply frequency($2f_1$)in the EPVA signature and the amplitude increases with the accretion of the shorted ratio.

A component $2sw_1$ less than the supply rotational frequency occurs in the airgap magnetomotive force (MMF) and it makes the three phase current component $2sw_1$ lower than the supply rotational frequency exist in stator windings. As a result of the modulation, motor torque oscillates along with the stator current pulsating,

therefore, the speed undulates with a frequency twice slip. The sideband at the frequency of $(1 \pm 2s)f_1$ is included in the spectrum of stator current [3,6] and the ratio between the amplitude of the sideband and the fundamental frequency current grade is directly correlated with the degree of broken bars. The simulating results indicate that the sideband whose amplitude is about 0.04 appear near the frequency of 42.9Hz thanks to two broken bars, which is very close to 0.05 near 43Hz in the experimental ending. As far as the location of sideband frequency is concerned, the simulating results is nearly same to the experimental ending, which is often the most important fault characteristic revealing the broken bar failure. It is a pity that the sideband amplitude in simulating results is a little lower than the experimental outcomes. The main reasons lie in that the test motor has operated long time and maybe have inherently electrical and mechanical imbalance or airgap eccentricity, etc. Additionally, simulating results reveal that the sideband magnitude is concerned with the number of broken bars. The more broken bars are, the more higher the sideband amplitude is. For example, the sideband amplitude is about 0.02 with one broken bar and 0.04 with two broken bars. It is clear that the failure severity can be judged by the ratio between the sideband amplitude and the fundamental frequency magnitude.

VI. CONCLUSION

This paper provides interior fault models for induction motors on the basis of the quantitative relation between

interior faults and stator or rotor impedances and uses the electro-magnetic transient simulation software EMTDC to verify them. From simulating results it is found that the frequency component 2sf(s is slip) lower than the fundamental frequency exists in the steady stator current and is correlated with the extension of failure. In addition, a spectral component at a frequency twice the fundamental supply frequency($2f_1$)in the EPVA signature occurs with shorted turns and also relates to the failure severity. Thus the models produced in this paper are acceptable qualitatively. Furthermore, by comparing with experimental outcomes the models are proven to be correct. Therefore, the study on interior faults penetrates into every turn of stator windings and every bar of rotor and the quantitative diagnosis study on interior faults of induction motors is realized. At the same time, the analytical model of induction motors with interior faults in EMTDC is enriched and the application function and field for EMTDC is also extended.

ACKNOWLEDGMENTS

REFERENCES

[1] Lin Liangzhen, Ye Lin. An Introduction to PSCAD/EMTDC, Power System Technology, 2000,24(1):p65-p66.

[2] H.W.Dommel, Translated by Li Yongzhuang, Lin Jiming, Zeng Zhaohua. EMTP theory book, Hydraulic And Electric Power Press, first edition, Aug. 1991, Beijing.

[3] F.Filippetti, G.Franceschini, M.Martelli, and C.Tassoni. Development of expert system knowledge base to on-line diagnosis of rotor electrical faults of induction motors. Industry Applications Society Annual Meeting, 1992. Conference Record of the 1992 IEEE, 1992,1:p92-p99.

[4] Chen Shikun. Design of machines, Mechanical Technology Publication.

[5] Sergio M.A.Cruz, A.J.Marques Cardoso. Stator Winding Fault Diagnosis in Three-Phase Synchronous and Asynchronous Motors, by the Extended Park's Vector Approach. IEEE Transactions on Industry Applications, 2001, 37(5):p1227–p1233.